DOI 10.1007/s10527-023-10289-5
Biomedical Engineering, Vol. 57, No. 3, September, 2023, pp. 159–163. Translated from Meditsinskaya Tekhnika, Vol. 57, No. 3, May–June, 2023, pp. 5–7
Original article submitted March 24, 2023

A Method and Device for Digital Diaphanoscopy for the Diagnosis of MS Pathologies

E. O. Bryanskaya* **and A. V. Dunaev**

A method and device for digital diaphanoscopy for the diagnosis of pathologies of the maxillary sinuses are addressed. A scheme for an experimental apparatus is presented and specialized medical and technical requirements for the device are described. The method was trialed in presumptively healthy volunteers and patients with MS pathologies. These studies led to development of a classification model based on linear discriminant analysis, which allows the presence of pathological changes in the maxillary sinuses to be detected with sensitivity and specificity indicators of 0.88 and 0.98 respectively.

Introduction

Diseases of the maxillary sinuses (MS) currently play a significant role in the world socioeconomic situation [1], and their incidence increases year on year [2]. Nasal endoscopy is an important method for diagnosis in the MS. However, this method only supports detection of the indirect signs of sinusitis, such as hyperemia, swelling of the nasal mucosa on the affected side, and narrowing of the lumen of the nasal passages [3]. The diagnostic value of ultrasound (US) in ENT applications is limited due to low accuracy, leading to a high rate of false positive diagnoses [4]. The use of radiography and computed tomography (CT) is limited because of radiation exposure of patients [3].

Optical imaging methods are currently in wide use [5]; these include digital diaphanoscopy [6]. Along with nasal endoscopy and ultrasound, diaphanoscopy is regarded as an economical diagnostic method and consists of probing the MS with safe, low-intensity radiation in the visible and near infrared spectrum (650 and 850 nm). In health, the MS is a air-filled cavity lined with a mucous membrane [7]. Probing radiation passing through the sinus is partially absorbed when pathological changes — purulent contents, cystic fluid, tumor formation, etc. — are present. Absorption of light is associated with high values for the coefficient of absorption of the MS with pathological changes due to presence of blood or absorbing exudates [8, 9]. Recording of diaphanograms therefore allows the presence or absence of pathological changes in the MS to be visualized.

Science and Technology Center for Biomedical Photonics, I. S. Turgenev Orel State University, Orel; E-mail bryanskayae@mail.ru.

*To whom correspondence should be addressed.

Previous studies have demonstrated the importance of not only quantitative assessment of diaphanograms, but also the development of a practical tool for real-time detection of the presence of pathological changes in the MS [10]. quantitative parameters determined using diaphanogram recordings can be used as diagnostic criteria for building a classification model [11], in particular, by linear discriminant analysis (LDA) [5].

Thus, the aim of the present work was to was to improve the quality of diagnosis of MS pathologies by developing a method and device for digital diaphanoscopy to detect pathology with a lower probability of false negative results.

Materials and Methods

The digital diaphanoscopy device developed here (Fig. 1) [10] was used in experimental studies with the participation of 49 presumptively healthy volunteers (13 men, 36 women, mean age 20 ± 3 years) and 42 patients with pathologies of the MS (20 men, 22 women, mean age 49 ± 17 years) with confirmation of diaphanoscopy results by reference methods (CT/MRI). Studies involving patients were carried out at the Department of Otorhinolaryngology, Clinical Center for Maxillofacial, Reconstructive, and Plastic Surgery, University Clinic, A. I. Evdokimov Moscow State University of Medicine and Dentistry (Moscow, Russia). After reading the study protocol, the volunteers signed informed consent indicating their readiness to participate in the study.

During investigations, the LED diaphanoscope applicator, operating at two probe wavelengths (650 and 850 nm), was placed in the patient's oral cavity for probing of

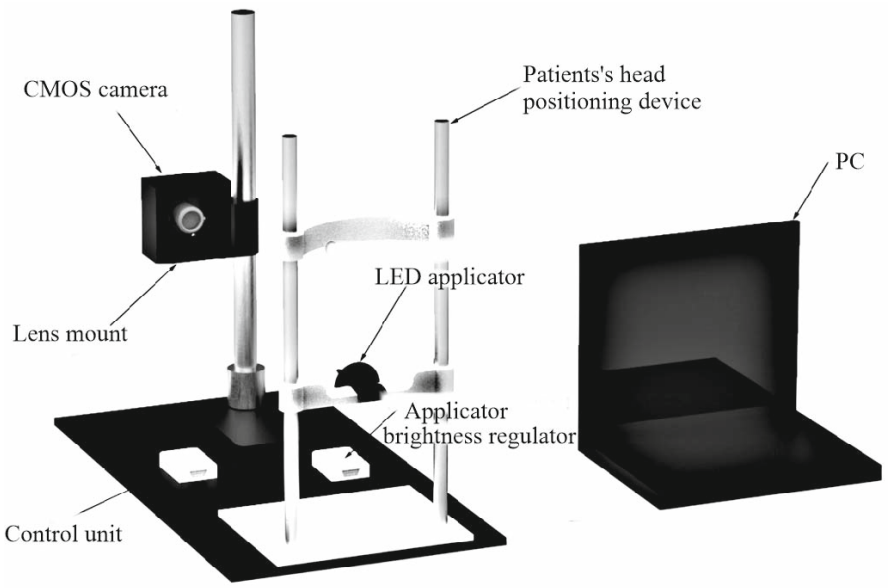

Fig. 1. Experimental arrangement for digital diaphanoscopy.

the MS. In accordance with evidence-based specialist medical and technical requirements [11], power levels for diagnosis in female patients were set to 25 and 65 mW, compared with 85 mW for male patients. Diaphanograms of size $N_x \times N_y$ (N_x = 1280, N_y = 1024) were then recorded using a UI-3240CP-NIR-GL Rev. 2 CMOS camera (Obersulm, Germany) with a Pentax C1614-M (KP) lens (Pentax, Japan) placed against the patient's face. The camera exposure time was set to 40 ms.

Each dot (pixel) on the diaphanogram records the light intensity reaching the camera detector after absorption and scattering in normal and/or pathologically altered MS tissues. The presence or absence of a pathological change is detected on the basis of the spatial distribution of light detected by the camera, determined, in particular, by the strong absorption of light at wavelengths of 650 and 850 nm in the area of the MS with pathology [8, 9].

Specially developed software provides control of device operation (selection of the radiation source and camera operation mode), diaphanogram recording, and qualitative (visualization) and quantitative (pseudostaining) processing, which consists of converting the diaphanogram $D(x, y)$ into an 8-bit image, which for convenience will

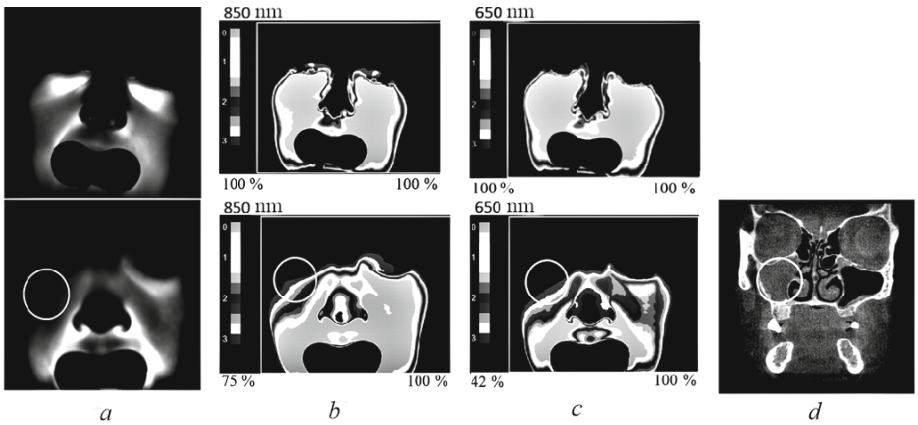

Fig. 2. An example of the results from investigation of a presumptively healthy volunteer (above) and a patient with mycetoma of the right MS (below): a) diaphanograms; b, c) pseudostaining with probe irradiation wavelengths of 850 and 650 nm respectively; d) CT of the upper and lower jaws in the coronal plane.

henceforth be presented on a percentage scale $I_n(x, y)$ as per Eq. (1):

$$I_n = \frac{D(x, y) - \min\limits_{x=1...N_x,\ y=1...N_y} D(x, y)}{\max\limits_{x=1...N_x,\ y=1...N_y} D(x, y) - \min\limits_{x=1...N_x,\ y=1...N_y} D(x, y)} \cdot 100\ \%. \quad (1)$$

Thus, depending on the extent of light absorption, pseudostaining provides visualization of the maxillary sinuses in the presence of pathological changes.

Results

Clinical Investigations

The healthy MS is filled with air due to the absence of pathological changes; as a result, no absorption of light occurs in the healthy MS, as confirmed by the digital diaphanoscopy results obtained from a presumptively healthy volunteer (Fig. 2, top). No absorption of light occurred in the left and right MS, indicating that they were filled with air and there were no pathological changes.

In the example from a patient (Fig. 2, bottom), both the diaphanogram and the pseudostaining results show darkening in the area of the right MS (the pathologically altered MS is marked with a white circle), which indicates a decrease in transparency and, thus, the presence of a pathological change (the left sinus is normal).

This example leads to the conclusion that pathological changes in the MS detected on CT can also be detected using the device developed for digital diaphanoscopy.

Application of LDA

In order to build a classification model to divide the study objects into two classes (healthy and pathological), quantitative parameters were calculated for diaphanogram recordings: the intensity parameter (*IP*) and the asymmetry coefficient (*CA*). The image *IP* is calculated by manually selecting the region of the maxillary sinuses (the region of interest, ROI), in which the average value of the light intensity is calculated using Eq. (2):

$$IP = \frac{\sum_{i=1...N} D_i}{N}, \quad (2)$$

where N is the number of pixels in the ROI.

Calculation of *CA* consists of determining the central line of the face (the axis of symmetry), rotating the diaphanogram to ensure that the central line is vertical, and calculating the coefficient of asymmetry between the left and right parts of the face. The calculation uses Equation (3):

$$CA = \frac{\sum_m \sum_n \left(A_{m,n} - \overline{A}\right)\left(B_{N_x/2-m,n} - \overline{B}\right)}{\sqrt{\sum_m \sum_n \left(A_{m,n} - \overline{A}\right)^2 \left[\sum_m \sum_n \left(B_{m,n} - \overline{B}\right)^2\right]}}, \quad (3)$$

where $A_{m,n} = D(x = 1...N_x/2,\ y = 1...N_y)$ and $B_{m,n} = D(x = N_x/2 + 1...N_x,\ y = 1...N_y)$ are the pixel intensities in the left and right parts of the diaphanogram respectively, and are the average intensities in the left and right parts of the diaphanogram respectively, and m and n are the numbers of rows and columns of the pixel matrix.

Analysis of the data obtained (Table 1) demonstrated a statistically significant difference between the indicators computed for presumptively healthy volunteers and patients with pathological changes in the MS.

A classification model based on LDA was built to divide the condition of the MS into two classes (with and without pathology) using *IP* and *CA* as diagnostic criteria. The classification model with the best values of sensitivity and specificity had the form

$$f = (\tau - 0.07IP) + (-7.26CA) + 9.85\ . \quad (4)$$

The results showed that sensitivity and specificity for the probe wavelength of 850 nm were 0.88 and 0.98 respectively ($AUC = 0.98$). These accuracy characteristics

TABLE 1. Results of statistical data processing

Probe wavelength	*IP*, rel. units		*CA*, rel. units	
	Normal	Pathology	Normal	Pathology
650 nm	113.80 [49.20; 222.30]	30.05 [0.10; 142.50]*	0.91 [0.74; 0.96]	0.62 [0.09; 0.86]*
850 nm	107.20 [37.40; 198.60]	27.85 [0.10; 100]*	0.89 [0.60; 0.96]	0.62 [0.08; 0.89]*

*Statistically significant difference between values, $p < 0.05$, Mann–Whitney test

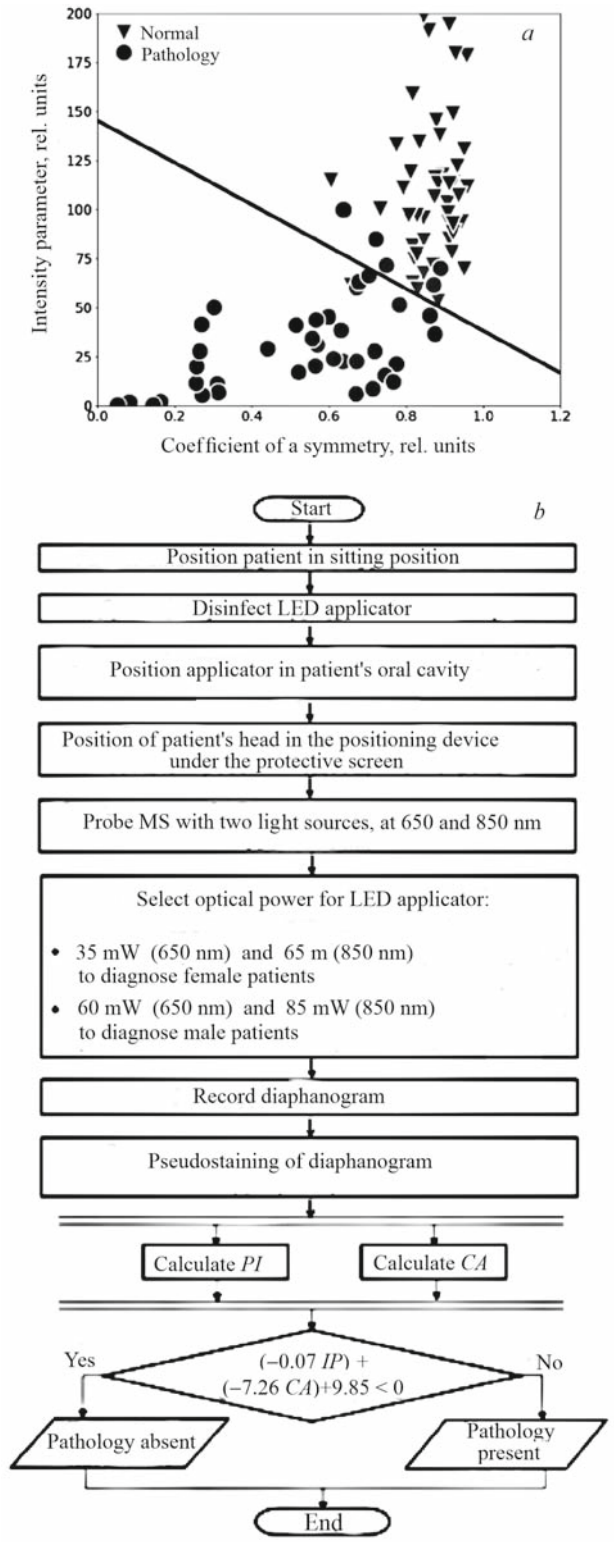

Fig. 3. Scatter plot of *IP* and *CA* values with application of the discriminant function (a); algorithm for digital diaphanoscopy for diagnosis of *MS* pathologies (b).

are greater than the sensitivity and specificity of nasal endoscopy and ultrasound [4], which indicates the great potential of the approach proposed here both for the rapid diagnosis of MS and for screening effectiveness.

The discriminant lines on the scatter plot of *IP* and *KA* values for the probe wavelength of 850 nm (Fig. 3a) divides the experimental points into two groups (healthy volunteers and patients). The classification model supported development of an algorithm for digital diaphanoscopy for diagnosis of MS pathologies (Fig. 3b).

After the direct diaphanogram recording stage, *IP* and *CA* are calculated and the classification model is applied to come to a conclusion regarding the presence or absence of MS pathology.

Conclusions

Thus, we present here a method and device developed for digital diaphanoscopy for the diagnosis of MS pathologies. Use of the proposed LDA-based classification allows the presence of pathology to be detected with high accuracy, with sensitivity and specificity of 0.88 and 0.98 respectively, which in turn reduces the likelihood of false negative results. Future work will improve the model developed here by enlarging the dataset and using it to develop a medical decision support system.

This study was carried out with the financial support of the Russian Foundation for Basic Research within the framework of scientific project No. 20-32-90147. We would like to thank the volunteers and patients of the University Clinic of A. I. Evdokimov Moscow State Medical University (Moscow, Russia) and doctors, Doctor of Medical Sciences D. N. Panchenkov, Master of Medical Sciences A. V. Bakotina, Master of Medical Sciences Yu. O. Nikolaeva, V. G. Pilnikova, and Doctor of Physical and Mathematical Sciences V. G. Artyushenk. ("Art photonics Ltd.," Berlin, Germany) for comprehensive assistance at all stages of the project.

REFERENCES

1. Ageenko, I. V. and Ageenko, L. I., "Medical polypotomy of the nasal cavity and paranasal sinuses using pit procedures," Folia Otorhinolaryngol. Pathol. Respir., **21**, No. 2, 10–13 (2015).
2. Shamsiev, D., Vokhidov, U., and Karimov, O., "Current views on the diagnosis and treatment of chronic inflammatory diseases of the nose and paranasal sinuses," Molodoi Uchenyi, No. 5, 84–88 (2018).

3. Shadyev, T. Kh., Izotova, G. N., and Sedinkin, A. A., "Acute sinusitis," Ross. Med. Zh., **21**, No. 11, 567–572 (2013).
4. Hsu, C. C., Sheng, C., and Ho, C. Y., "Efficacy of sinus ultrasound in diagnosis of acute and subacute MSitis," J. Chinese Med. Assoc., **81**, No. 10, 898–904 (2018).
5. Dunaev, A. V., Multimodal Optical Diagnostics of Microcirculatory Tissue Systems of the Human Body. A Monograph [in Russian], TNT, Staryi Oskol (2022).
6. Stoelzel, K., Szczepek, A. J., Olze, H., Koss, S., Minet, O., and Zabarylo, U., "Digital diaphanoscopy of the MSes: A revival of optical diagnosis for rhinosinusitis," Am. J. Otolaryngol., **41**, No. 3, Article ID 102444 (2020).
7. Al-Qahtani, A., Haidar, H., and Larem, A., Textbook of Clinical Otolaryngology, Springer Nature (2020).
8. Peters, V. G., Wyman, D. R., Patterson, M. S., and Frank, G. L., "Optical properties of normal and diseased human breast tissues in the visible and near infrared," Phys. Med. Biol., **35**, No. 9, 1317–1334 (1990).
9. Van Veen, R., Sterenborg, H. J. M., Marinelli, A. W., and Menke-Pluymers, M. B. E., "Intraoperatively assessed optical properties of malignant and healthy breast tissue used to determine the optimum wavelength of contrast for optical mammography," J. Biomed. Opt., **9**, No. 6, 1129–1136 (2004).
10. Bryanskaya, E. O., Novikova, I. N., Dremin, V. V., Gneushev, R. Y., Bibikova, O. A., Dunaev, A. V., and Artyushenko, V. G., "Optical diagnostics of the MSes by digital diaphanoscopy technology," Diagnostics (Basel), **11**, No. 77, 1–13 (2021).
11. Bryanskaya, E. O., Novikova, I. N., Dremin, V. V., Nikolaeva, Yu. O., Pil'nikov, V. G., Bakotina, A. V., Ovchinnikov, A. Y., Panchenkov, D. N., Baranov, A. V., Artyushenko, V. G., and Dunaev, A. V., "Digital diaphanoscopy in the diagnosis of MS diseases for patients with different anatomical and gender features," Proc. SPIE, **12192**, Article ID 121920A (2022).